Assessment of pH-responsive nanoparticles performance on laboratory column flotation cell applying a real ore feed

N.B. When citing this work, cite the original published paper.

(article starts on next page)

Assessment of pH-responsive nanoparticles performance on laboratory column flotation cell applying a real ore feed

Samiramis Nasirimoghaddam [a], Ali Mohebbi [a,*], Mohsen Karimi [b], M. Reza Yarahmadi [c]

[a] Department of Chemical Engineering, Faculty of Engineering, Shahid Bahonar University of Kerman, Kerman, Iran
[b] Department of Chemistry and Chemical Engineering, Chalmers University of Technology, SE-41296 Gothenburg, Sweden
[c] Sarcheshmeh Copper Complex, Kerman, Iran

ABSTRACT

Nanoparticles (NPs) can promote the column flotation process in mining industry. Nanoparticles' effects on column flotation process (copper recovery, grade and flotation rate constant) are assessed in Sarcheshmeh Copper Complex, Iran, through response surface methodology (RSM) optimization technique. The γ-Al_2O_3, α-Fe_2O_3, SiO_2, and TiO_2 nanoparticles are selected for these experiments. A flotation rate constant is chosen as a response to assess the effect of nanoparticles on flotation in its kinetic sense. The process pH and nanoparticle dosage are selected as the influential parameters. Results obtained from RSM indicated that the maximum percentage of Cu recovery and grade is obtained at pH of 12 and nanoparticle dosage of 6 kg/t, through α-Fe_2O_3 and γ-Al_2O_3 nanoparticles, respectively. Applying nanoparticles in particular γ-Al_2O_3 and α-Fe_2O_3 increases the Cu recovery by 8–10% together with the grade by 3–6% in a significant manner. It is revealed that nanoparticles could effectively be applied in enhancing the flotation performance.

1. Introduction

Flotation is one of the most effective techniques applied widely in separating copper ore based on their differences in physical and chemical properties. In this process, after preparing the pulp with chemical reagents, named collectors, it is revealed that some of them are hydrophobic and some hydrophilic. In the selected separation processes, copper minerals attach to air bubbles and move to the surface of the flotation cell and form a stable froth layer containing 20–30% copper. The column flotation is one of the latest flotation methods with a high focus in mineral processing. In general, due to its simpler structure, higher selectivity, low cost, better product recovery and higher grade, it is more efficient than the conventional flotation cells [1–6].

It is found that the flotation performance (i.e. recovery and grade) strongly depends on the froth stability, bubble distribution, bubble mobility and froth properties on which there exit many studies, e.g. [7–10]. If the froth is too stable, then detachment of affixed material from the froth is difficult, otherwise, the floated material is lost due to the bubble coalescence in the froth. The run assessments indicate that in addition to the type and concentration of the frother, the hydrophobicity, particle size, type and concentration of present particles affect the froth stability and cause an increase in the hydrophobic particles, leading to an increase in froth stability [11–17].

To improve the froth stability in mineral products in the related industries, it is necessary to apply new technologies. Nanotechnology is one of these growing and important technologies with widespread applications in mineral processing worldwide. Because of nanoparticles' distinct properties and their high surface to volume ratio, they are able to promote the froth stability, and enhance the flotation performance. In addition, nanoparticles (NPs) are demonstrated to play an important role as the effective collector in flotation process [18–22]. Nanoparticles are of great potential applications in flotation field and are applied as a stabilising agent, like surfactant to enhance the froth stability by retarding bubble coalescence. The ability of the nanoparticles to stabilize froth on its own and without any other surfactant is the subject of many studies not related to flotation processing. These studies indicate that the nanoparticles increase the froth stability by forming a barrier to coalescence and decelerating the process of thinning the film though preventing the water flow at the bubble surface [19,23]. Nanoparticles are recyclable, thus profitable [24–26].

Despite some studies run on nanoparticle-stabilized froth, studies on nanoparticles in the three-phase column flotation with an

industrial feed are limited and yet the nanotechnology can be applied in the mineral separation which is a new challenge [27,28]. The simultaneous effects of different parameters including process environment pH and NP dosage on copper recovery, grade and flotation rate constant are not assessed enough. Reviews run by the authors here indicate that only a single mineral in the flotation process has been subject of study. To study the simultaneous effects of important parameters, one of the statistical techniques, response surface methodology (RSM), is usually applied [29,30].

The RSM is applied for analyzing experiments where one or more independent variables–as responses–are affected by many variables with the objective to optimize the responses [31,32]. One of the advantages of applying RSM in the Design Expert software environment, in addition to reducing the number of experiments, is the possibility of devising equations for independent and dependent variables. The RSM includes different design models like Box-Behnken (BB), factorial, D-optimal, and central composite design (CCD) [30,33,34]. This method is successfully applied in optimizing different processes to reduce the cost of analysis methods like computational fluid dynamics (CFD) and their related numerical uncertainties [35–38].

Here, the usability of nanoparticle stabilized froth is assessed through RSM technique based on CCD approach in a flotation process. To materialize this objective here, the simultaneous effects of critical parameters like the process pH and NP dosage on the flotation performance responses are assessed. In this study, assessing the flotation rate constant (k) is the main subject of the flotation kinetics because it is presented as a function of the flotation dynamics and the properties of minerals. In addition to the recovery and grade, assessing the flotation rate constant is of essence [39]. Assessing the effect of these nanoparticles on the recovery, grade and flotation rate constant for an industrial feed is new. To assure the size of selected nanoparticles, the dynamic light scattering (DLS) is applied.

2. Materials and methods

The method adopted in this study is experimental. The flotation column is devised in the Sarcheshmeh Copper Complex laboratory. Efforts are made to assess the possibility of applying nanoparticles as a platform for the progress of column flotation both in their quantitative (recovery) and qualitative (grade) sense in real ore flotation.

2.1. Experimental system

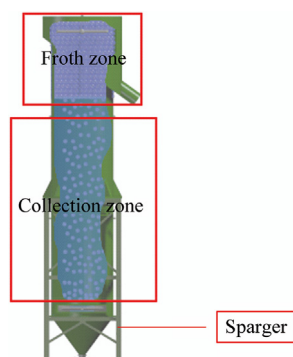Batch flotation experiments are designed through RSM to assess the effects of critical factors on the flotation performance. The experiments are run on a laboratory-scale flotation column setup (Fig. 1).

Based on the aspect ratios of the pilot plant and industrial flotation columns, a 0.007 m^3 flotation column is designed and built. This column is cylindrical and to see the pulp level easily, and is made of transparent Plexiglass. The dimensions of the column are 10 cm diameter and 100 cm height. Water is added to maintain the level of the pulp in the column and the tests are run to reduce the froth depth. A porous polyethylene cylinder is installed at the bottom of the column to distribute air over the column cross-section in a uniform manner with a filter cloth sparger.

The subject copper ore samples are processed in the flotation column with constantly adding reagent at any process. Here, first, the nanoparticle is dispersed by the agitator into 7.5% constant solid pulp. Next, the collector dosages (sodium isopropyl xanthate and butyl sodium dithiphosphate) are added into the pulp to enhance the hydrophobicity of copper particles and to allow 2 min for conditioning. Then, the frother dosages (MIBC and Nas-froth) are added and conditioned for a further 1 min. These flotation conditions are determined by applying the results of the preliminary flotation tests performed without the nanoparticles. Finally, air is injected through the flowmeter with the superficial gas velocity of 1.5 cm/s at the bottom of the column and the concentrates' collection is accomplished at 0.5, 1.5, 4 and 8 min cumulative times into separate containers with tailings that are filtered, dried and weighed. Here the process pH of tests is adjusted by adding CaO. The Laser Particle Sizer (FRITSCH ANALYSETTE 22 Nano-Tec) is applied to measure the mineral particle size. In this study, the froth depth is kept constant at 4 cm in all runs.

The flotation rate constant (k) as the indicator of flotation performance, is subject to both the dynamics of flotation columns and the chemical properties of the minerals, which are determined by fitting the following first-order rate equation to the recovery-time curves obtained for each particle size fraction [40]:

$$R = R_{max}(1 - \exp(-kt)) \tag{1}$$

where R_{max} is the predicted maximum recovery.

The four nanoparticles types of γ-Al$_2$O$_3$, α-Fe$_2$O$_3$, SiO$_2$, and TiO$_2$ were purchased from US Research Nanoparticles, Inc., USA and applied in the designed flotation experiments. Their properties are tabulated in Table 1.

2.2. Experiment design

In this experiment, the flotation experiments are optimized through a three-level (-1, 0, $+1$) and two-parameter CCD approach in Design Expert V 10.0.3 S/W. Selected parameters and their levels are determined from the obtained results of preliminary tests. The parameters considered here consist of the process pH (X_1) and NP dosage (X_2) as the independent parameters, being the most influenced on the flotation process. The available results indicate that the copper recoveries remain relatively high in the alkaline pH range and the highest recovery and grade are yielded with pH in the range of 10–12 [2]; thus, this range was selected for flotation experiments. The applied industrial samples are of pyrite minerals that are naturally depressed at alkaline pH > 10, indicating that selective separation of copper from samples can be achieved at

Fig. 1. Schematic of the laboratory flotation column of the Sarcheshmeh Copper Complex.

Table 1
Nanoparticles applied in this study.

Nanoparticle	Particle size (nm)	Purity (%)
γ-Al$_2$O$_3$	20	>99
α-Fe$_2$O$_3$	20–40	>98
SiO$_2$	11–13	>99
TiO$_2$	10–25	>99

pH > 10, thus causing an increase in the grade. In our experiment design, the changes in NP dosage are assessed within the range of 0.5–10 kg/t. The results (Fig. 2) showed that recovery variations from dosage of 0.5–2 kg/t are negligible. An increase in NP dosage (with the range of 4–10 kg/t) increases the recovery percentage, but in the range of 6–10 kg/t these percentages are close to each other; therefore here, a 4–6 kg/t range is selected for the four applied NPs.

The copper recovery (Y_1), copper grade (Y_2) and flotation rate constant (Y_3) are applied as the response variables. The levels of the independent and dependent selected variables are tabulated in Tables 2 and 3, respectively. For each NP, a total of 17 experiments consisting of five replicates at the centre points, one axial point and two full factorial points with three responses are designed and implemented in one block in a random manner.

The reliable approach in evaluating the accuracy of the fitted model is assessed by the coefficient of determination (p-value and R^2), the lack of fit tests and the Fisher test value (F value) obtained from ANOVA. The graphical analysis is run to illustrate the optimum condition for column flotation performance. The objective of this design is to assess the optimal pH and NP dosage for improving the column flotation performance.

3. Results and discussion

3.1. Dynamic light scattering (DLS)

The hydrodynamic diameter distribution of the four NP types in water at 90° fixed scattering angle and 25 °C constant temperature prepared by the dynamic light scattering (DLS-HORIBA L-550) technique is applied to confirm the hydrodynamic NPs size. The size distributions for the subject NPs are nano-sized, Fig. 3, where,
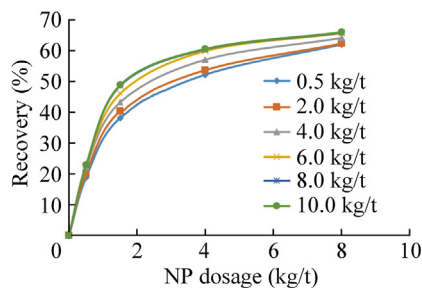

Fig. 2. Effect of NP dosage on recovery.

Table 2
Levels of independent variables in the CCD experimental design.

Independent variables	Code units	Coded levels		
		−1	0	1
Process pH	X_1	10	11	12
NP dosage (kg/t)	X_2	4	5	6

Table 3
Selected dependent variables in the CCD experimental design.

Dependent variables (response)	Code units
Cu recovery (%)	Y_1
Cu grade (%)	Y_2
Cu flotation rate constant (1/min)	Y_3

as observed it is confirmed that the distribution range of the subject NPs in Table 1 is narrow.

3.2. Design of experiment

The experiments are run according to CCD approach of the RSM to optimize the nanoparticles' conditions in obtaining maximum column flotation performance through nanoparticles in 17 batch runs for every nanoparticle. Details of the nanoparticles in the design of experiment are tabulated in Tables 4–7.

The obtained results through Design Expert software are represented as ten quadratic polynomial and two linear equations of Y_3 model for γ-Al$_2$O$_3$ and TiO$_2$ for predicting all three responses:

For γ-Al$_2$O$_3$ NPs:

$$Y_1 = 59.93 + 5.48X_1 + 1.77X_2 + 0.95X_1X_2 + 0.78X_1^2 + 0.43X_2^2 \tag{2}$$

$$Y_2 = 23.18 + 5.05X_1 + 1.37X_2 + 0.45X_1X_2 - 0.37X_1^2 + 0.13X_2^2 \tag{3}$$

$$Y_3 = 1.25 - 0.50X_1 + 0.18X_2 \tag{4}$$

For α-Fe$_2$O$_3$ NPs:

$$Y_1 = 62.53 + 5.75X_1 + 0.75X_2 + 3.20X_1X_2 - 2.47X_1^2 + 1.53X_2^2 \tag{5}$$

$$Y_2 = 22.66 + 2.70X_1 - 0.34X_2 + 0.23X_1X_2 + 1.11X_1^2 + 0.71X_2^2 \tag{6}$$

$$Y_3 = 1.01 - 0.37X_1 + 0.16X_2 + 0.023X_1X_2 + 0.021X_1^2 + 0.12X_2^2 \tag{7}$$

For SiO$_2$ NPs:

$$Y_1 = 62.69 + 5.90X_1 + 1.32X_2 - 0.05X_1X_2 - 4.13X_1^2 - 0.03X_2^2 \tag{8}$$

$$Y_2 = 21.30 + 4.40X_1 + 0.89X_2 + 0.12X_1X_2 - 0.92X_1^2 + 0.33X_2^2 \tag{9}$$

$$Y_3 = 0.84 - 0.32X_1 - 0.12X_2 + 0.056X_1X_2 + 0.13X_1^2 + 0.012X_2^2 \tag{10}$$

And for TiO$_2$ NPs:

$$Y_1 = 64.80 + 0.72X_1 + 1.80X_2 - 0.15X_1X_2 - 11.11X_1^2 - 0.51X_2^2 \tag{11}$$

$$Y_2 = 23.03 + 3.28X_1 + 1.16X_2 + 0.52X_1X_2 - 0.59X_1^2 + 0.11X_2^2 \tag{12}$$

$$Y_3 = 0.87 - 0.36X_1 - 0.08X_2 \tag{13}$$

where X_1 is the process pH; X_2 the NP dosage; and X_1X_2 the interaction of these two parameters.

The X_1X_2 is the response changes when two independent variables (X_1 and X_2) are changed simultaneously. The positive and negative signs of coefficient indicate the positive and negative effect on Y_1, Y_2 and Y_3. An increase in the pH with the range of 10–12 decreases the flotation rate constant in the chalcopyrite samples; X_1 has negative impacts on the response Y_3, for every nanoparticle. This may be due to the factors like nanoparticle aggregation, changing the pulp viscosity or longer bubble resistance time.
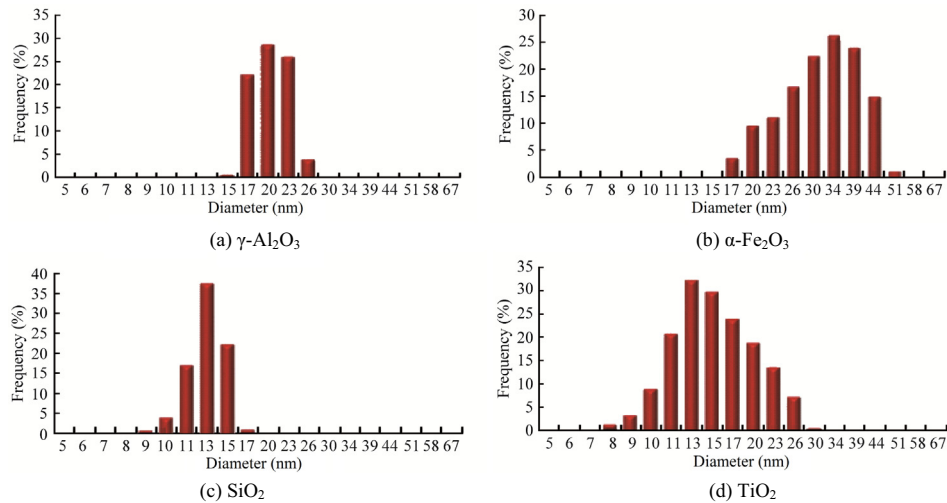
(a) γ-Al$_2$O$_3$

(b) α-Fe$_2$O$_3$

(c) SiO$_2$

(d) TiO$_2$

Fig. 3. DLS graphs of the four NPs.

Table 4
Experimental design of the column flotation and obtained results for γ-Al$_2$O$_3$.

Run	X_1		X_2 (kg/t)		Y_1 (%)	Y_2 (%)	Y_3 (1/min)
	Coded	Actual	Coded	Actual			
1	0	11	0	5	59.0	22.0	1.40
2	−1	10	−1	4	55.0	15.8	1.62
3	0	11	0	5	60.0	23.0	1.33
4	+1	12	0	5	65.0	27.0	0.71
5	+1	12	+1	6	69.2	26.0	0.87
6	+1	12	−1	4	64.5	25.8	0.55
7	0	11	0	5	60.0	22.5	1.30
8	−1	10	−1	4	54.5	16.5	1.60
9	−1	10	+1	6	55.6	17.8	1.89
10	+1	12	−1	4	64.0	24.5	0.58
11	0	11	0	5	60.3	22.0	1.24
12	0	11	0	5	61.0	23.0	1.20
13	−1	10	0	5	55.8	17.5	1.70
14	0	11	−1	4	58.1	20.0	0.93
15	+1	12	+1	6	70.0	30.0	0.91
16	0	11	+1	6	62.0	24.0	1.52
17	−1	10	+1	6	57.0	17.0	1.85

Table 5
Experimental design of the column flotation and obtained results for α-Fe$_2$O$_3$.

Run	X_1		X_2 (kg/t)		Y_1 (%)	Y_2 (%)	Y_3 (1/min)
	Coded	Actual	Coded	Actual			
1	0	11	+1	6	64.0	24.69	1.30
2	0	11	−1	4	62.5	23.67	0.88
3	+1	12	−1	4	63.0	27.26	0.55
4	0	11	0	5	62.7	22.17	1.01
5	0	11	0	5	63.0	23.00	1.09
6	0	11	0	5	62.0	22.00	1.11
7	−1	10	−1	4	60.0	22.422.41	1.45
8	−1	10	−1	4	58.0	22.30	1.40
9	−1	10	0	5	51.5	21.91	1.25
10	+1	12	+1	6	72.0	26.30	0.93
11	−1	10	+1	6	54.2	21.58	1.65
12	+1	12	−1	4	63.2	27.36	0.60
13	0	11	0	5	64.0	22.60	0.90
14	0	11	0	5	62.6	21.90	0.99
15	+1	12	+1	6	70.0	27.00	0.92
16	+1	12	0	5	67.0	27.26	0.74
17	−1	10	+1	6	54.0	20.00	1.72

Table 6
Experimental design of the column flotation and obtained results for SiO_2.

Run	X_1		X_2 (kg/t)		Y_1 (%)	Y_2 (%)	Y_3 (1/min)
	Coded	Actual	Coded	Actual			
1	0	11	+1	6	63.2	23.7	0.78
2	0	11	−1	4	62.0	22.3	0.99
3	+1	12	−1	4	63.0	24.2	0.71
4	0	11	0	5	62.0	22.8	0.80
5	0	11	0	5	63.0	23.0	0.84
6	0	11	0	5	62.0	23.1	0.79
7	−1	10	−1	4	52.0	18.4	1.50
8	−1	10	−1	4	50.0	18.7	1.42
9	−1	10	0	5	53.0	19.0	1.35
10	+1	12	+1	6	65.0	27.5	0.58
11	−1	10	+1	6	54.2	20.3	1.06
12	+1	12	−1	4	63.2	23.9	0.73
13	0	11	0	5	64.0	23.0	0.82
14	0	11	0	5	62.6	23.5	0.85
15	+1	12	+1	6	67.0	27.8	0.60
16	+1	12	0	5	64.0	25.6	0.66
17	−1	10	+1	6	54.0	19.8	1.15

Table 7
Experimental design of the column flotation and obtained results for TiO_2.

Run	X_1		X_2 (kg/t)		Y_1 (%)	Y_2 (%)	Y_3 (1/min)
	Coded	Actual	Coded	Actual			
1	0	11	+1	6	68.2	23.50	0.72
2	0	11	−1	4	60.0	20.00	0.97
3	+1	12	−1	4	53.0	24.50	0.55
4	0	11	0	5	65.0	20.77	0.80
5	0	11	0	5	64.5	21.00	0.88
6	0	11	0	5	64.8	20.81	0.85
7	−1	10	−1	4	51.2	16.00	1.20
8	−1	10	−1	4	51.0	15.50	1.35
9	−1	10	0	5	52.9	16.00	1.29
10	+1	12	+1	6	55.1	26.00	0.43
11	−1	10	+1	6	54.0	16.70	1.20
12	+1	12	−1	4	52.8	24.00	0.62
13	0	11	0	5	64.9	22.17	0.90
14	0	11	0	5	65.2	21.50	0.88
15	+1	12	+1	6	55.0	25.70	0.43
16	+1	12	0	5	54.1	25.00	0.55
17	−1	10	+1	6	53.7	17.00	1.11

To evaluate the accuracy of these models for each nanoparticle, the criteria of R^2 and adjusted R^2 coefficient, SD, CV and AP values are applied. The results reveal that these models can estimate the recovery, grade and flotation rate constant of copper, in a sufficient manner.

3.3. ANOVA analysis

Results of the fitted models of responses obtained through ANOVA analysis are tabulated in Tables 8–11 for γ-Al_2O_3, α-Fe_2O_3, SiO_2, and TiO_2 NPs, respectively, where, these suggested models are significant at 95% confidence level (p-value < 0.05) in predicting copper recovery, grade and flotation rate constant.

As shown in Tables 8–11, all model F-values' amounts for copper recovery, copper grade and flotation rate constant parameters are high for all subject NPs, indicating that the models are highly significant and there is only a 0.01% chance for the model F-value distribution, which is due to noise. The $Prob > F$ values less than 0.05 indicate that the model terms are significant for all NPs, and the highly significant models are observed at the 95% confidence level.

The low amounts of lack of fit of suggested models, that describe the variation of the data around the presented models, are not significant, indicating the fitness of the models. The results indicate that $R^2 > 0.9$ for all suggested models of the four NPs is of appropriate fit of the models to the experimental data. The adjusted R^2 values for all response models are higher than 0.9, except Y_2 for α-Fe_2O_3 which is about 0.88. These findings confirm that these models are appropriate for predicting the responses in all four NPs.

The AP values measure the signal to noise ratio, where $AP > 4$ is appropriate, and here, the $AP > 4$ holds true in all presented models for all NPs. This value suggests that these models can be applied in navigating the design space. For these models to be reproduced the CV values must not exceed 10% [41]. Accordingly, the CV values of these three responses are within the range of 1.06–6.11% for γ-Al_2O_3, 2.16–7.81% for α-Fe_2O_3, 1.46–4.63% for SiO_2 and 1.42–5.92% for TiO_2 NPs, indicating a reliable precision and reliability of these models.

3.4. Response surface analysis

To assess the interaction and the simultaneous effects of different independent parameters on the responses, the 3D response surface graphs are plotted in Fig. 4a–d, Fig. 5a–d and Fig. 6a–d for Cu recovery, Cu grade and Cu flotation rate constant, with different NPs, respectively.

Table 8
ANOVA results for Cu recovery (Y_1), grade (Y_2) and flotation rate constant (Y_3) for γ-Al$_2$O$_3$.

	Y_1 (%)			Y_2 (%)			Y_3 (1/min)		
	Mean square	F value	p-value, Prob > F	Mean square	F value	p-value, Prob > F	Mean square	F value	p-value, Prob > F
Model	68.71	122.60	<0.0001	55.17	929.37	<0.0001	1.42	245.58	<0.0001
X_1	300.30	535.80	<0.0001	255.03	4296.10	<0.0001	2.54	437.78	<0.0001
X_2 (kg/t)	31.33	55.90	<0.0001	18.77	316.18	<0.0001	0.31	53.39	<0.0001
X_1X_2 (kg/t)	7.22	12.88	0.0042	1.62	27.29	0.0003			
X_1^2	1.85	3.30	0.0967	0.42	7.01	0.0227			
X_2^2 (kg/t)	0.56	1	0.3378	0.051	0.85	0.3757			
Lack of fit	0.85	1.87	0.2126	0.097	2.14	0.1729	9.110E−3	2.74	0.0941
Pure error	0.45			0.045			3.321E−3		
SD	0.75			0.24			0.076		
Mean	60.65			23.04			1.25		
CV (%)	1.23			1.06			6.11		
AP	32.602			88.707			42.501		
R^2	0.9824			0.9976			0.9723		
Adjusted R^2	0.9744			0.9966			0.9683		

Table 9
ANOVA results for Cu recovery (Y_1), grade (Y_2) and flotation rate constant (Y_3) for α-Fe$_2$O$_3$.

	Y_1 (%)			Y_2 (%)			Y_3 (1/min)		
	Mean square	F value	p-value, Prob > F	Mean square	F value	p-value, Prob > F	Mean square	F value	p-value, Prob > F
Model	87.38	48.76	<0.0001	16.97	24.34	<0.0001	0.35	48.07	<0.0001
X_1	330.63	184.49	<0.0001	72.79	104.40	<0.0001	1.39	193.04	<0.0001
X_2 (kg/t)	5.63	3.14	0.1041	1.18	1.69	0.2205	0.27	37.32	<0.0001
X_1X_2 (kg/t)	81.92	45.71	<0.0001	0.41	0.59	0.4596	4.050E−3	0.56	0.4692
X_1^2	18.46	10.30	0.0083	3.75	5.38	0.0407	1.365E−3	0.19	0.6719
X_2^2 (kg/t)	7.10	3.96	0.0720	1.52	2.18	0.1683	0.041	5.68	0.0363
Lack of fit	4.51	5.82	0.0207	1.77	6.05	0.0187	0.015	3.66	0.0630
Pure error	0.77			0.29			4.175E−3		
SD	1.34			0.84			0.085		
Mean	61.98			23.73			1.09		
CV (%)	2.16			3.52			7.81		
AP	22.507			12.539			21.295		
R^2	0.9568			0.9171			0.9562		
Adjusted R^2	0.9372			0.8794			0.9363		

Table 10
ANOVA results for Cu recovery (Y_1), grade (Y_2) and flotation rate constant (Y_3) for SiO$_2$.

	Y_1 (%)			Y_2 (%)			Y_3 (1/min)		
	Mean square	F value	p-value, Prob > F	Mean square	F value	p-value, Prob > F	Mean square	F value	p-value, Prob > F
Model	87.26	112.59	<0.0001	40.86	121.84	<0.0001	0.25	139.53	<0.0001
X_1	348.10	449.12	<0.0001	193.60	577.27	<0.0001	1.02	563.99	<0.0001
X_2 (kg/t)	17.42	22.48	0.0006	7.92	23.62	0.0005	0.14	76.69	<0.0001
X_1X_2 (kg/t)	0.020	0.026	0.8753	0.13	0.37	0.5539	0.025	13.94	0.0033
X_1^2	51.66	66.66	<0.0001	2.57	7.67	0.0182	0.052	28.85	0.0002
X_2^2 (kg/t)	2.760E−3	3.561E−3	0.9535	0.33	0.97	0.3451	4.012E−4	0.22	0.6475
Lack of fit	0.57	0.67	0.5924	0.65	3.00	0.0950	3.241E−3	2.53	0.1308
Pure error	0.85			0.22			1.281E−3		
SD	0.88			0.58			0.043		
Mean	60.25			20.95			0.92		
CV (%)	1.46			2.76			4.63		
AP	27.609			30.752			34.605		
R^2	0.9808			0.9823			0.9845		
Adjusted R^2	0.9721			0.9742			0.9774		

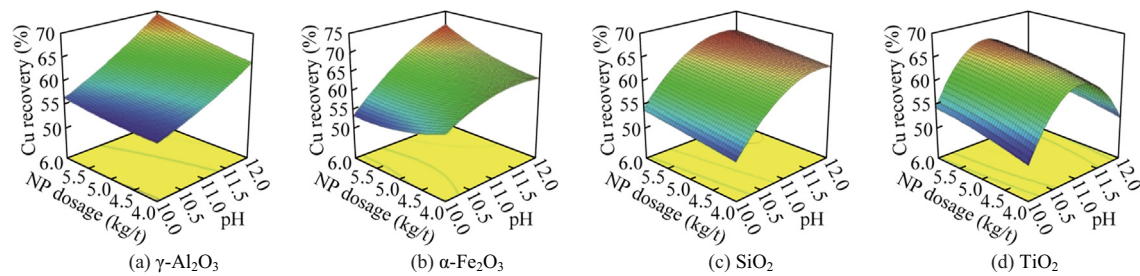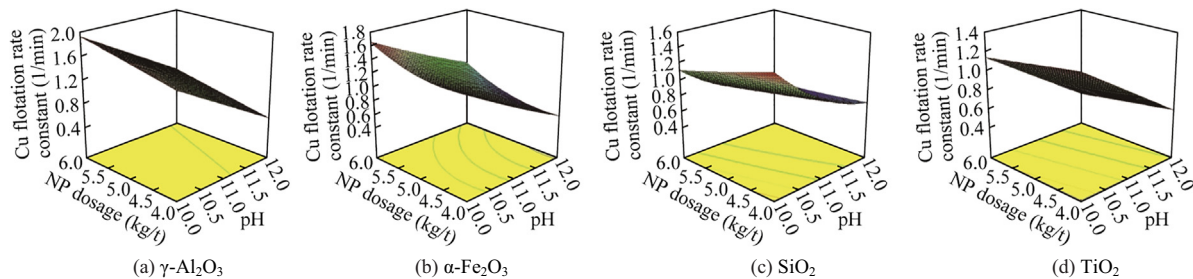### 3.4.1. Effect of pH and NP dosage on the Cu recovery

As to Cu recovery, the 3D simultaneous effects of process pH and NP dosage for γ-Al$_2$O$_3$, α-Fe$_2$O$_3$, SiO$_2$ and TiO$_2$ NPs are shown in Fig. 4a–d, respectively, whereas observed, this recovery depends more on the pH than the NP dosage, thus making pH the most effective parameter. Recovery increases by an increase in both the parameters for all NPs (except for TiO$_2$). This dependency on pH can be attributed to its performance on NPs. Because NPs stabilize the froth with their large surface area; an increase in the NPs concentration produce smaller bubble and bigger surface area, thus causing an increase in recovery. Accordingly, any amount of NP dosage indicates a positive effect on recovery for all NPs. As observed in Fig. 4d, as to TiO$_2$ the effect of pH and NP dosage on the Cu recovery are positive until the pH pulp reaches 11, after which a decreasing trend is followed as the pulp pH increase. This phenomenon indicates that by increasing pH (with the range of 11–12) the bubble coalescence in the froth on the surface decrease in presence of TiO$_2$ which is directly related to drainage of the

Table 11
ANOVA results for Cu recovery (Y_1), grade (Y_2) and flotation rate constant (Y_3) for TiO_2.

	Y_1 (%)			Y_2 (%)			Y_3 (1/min)		
	Mean square	F value	p-value, Prob > F	Mean square	F value	p-value, Prob > F	Mean square	F value	p-value, Prob > F
Model	114.31	91.04	<0.0001	24.89	237.47	<0.0001	0.67	253.93	<0.0001
X_1	5.18	4.13	0.0670	107.58	1026.29	<0.0001	1.27	483.57	<0.0001
X_2 (kg/t)	32.40	25.80	0.0004	13.46	128.36	<0.0001	0.064	24.28	0.0002
X_1X_2 (kg/t)	0.18	0.14	0.7122	2.20	21.03	0.0008			
X_1^2	374.04	297.90	<0.0001	1.06	10.14	0.0087			
X_2^2 (kg/t)	0.80	0.64	0.4423	0.035	0.33	0.5749			
Lack of fit	4.48	100.21	0.0289	0.21	3.16	0.0860	2.178E−3	0.73	0.6386
Pure error	0.045			0.066			2.979E−3		
SD	1.12			0.32			0.051		
Mean	57.96			22.74			0.87		
CV (%)	1.93			1.42			5.92		
AP	23.409			46.166			40.526		
R^2	0.9764			0.9908			0.9732		
Adjusted R^2	0.9657			0.9866			0.9693		

(a) γ-Al₂O₃ (b) α-Fe₂O₃ (c) SiO₂ (d) TiO₂

Fig. 4. Response surface plots showing the effects of pH and NP dosage on Cu recovery for different NPs.

(a) γ-Al₂O₃ (b) α-Fe₂O₃ (c) SiO₂ (d) TiO₂
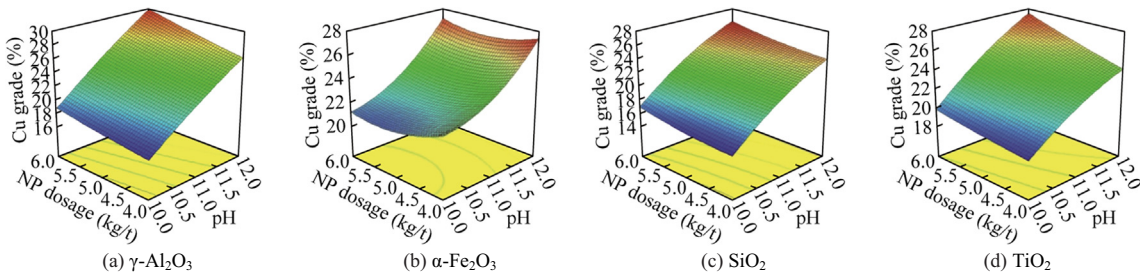
Fig. 5. Response surface plots showing the effects of pH and NP dosage on Cu grade for different NPs.

(a) γ-Al₂O₃ (b) α-Fe₂O₃ (c) SiO₂ (d) TiO₂

Fig. 6. Response surface plots showing the effects of pH and NP dosage on Cu flotation rate constant for different NPs.

liquid available in the bubbles which ultimately reduce recovery. As observed in Fig. 4d, the presence of TiO_2 has a positive effect and by an increase in NP dosage increases recovery.

3.4.2. Effect of pH and NP dosage on the Cu grade

The 3D surface plots of the two parameters' effects on the Cu grade for γ-Al_2O_3, α-Fe_2O_3, SiO_2 and TiO_2 NPs are shown in Fig. 5a–d, respectively. Fig. 5a–d reveal the synergistic effect for both the parameters while pH has the greatest influence on Cu grade and a slight effect of the NP dosage is observed on the α-Fe_2O_3 grade. The copper grade gradually increases with an increase in the pH for all NPs. The percentage grade increases with an increase in γ-Al_2O_3, SiO_2 and TiO_2 NP dosage. This finding is in agreement with the p-values in Tables 8–11 obtained from ANOVA analysis.

3.4.3. Effect of pH and NP dosage on flotation rate constant

The combined effects of the two independent parameters on flotation rate constant for γ-Al_2O_3, α-Fe_2O_3, SiO_2 and TiO_2 NPs are presented in Fig. 6a–d, respectively. The drown plots reveal that pH has a greater influence on flotation rate constant than dosage. Both the parameters exhibit a similar impact on the flotation rate constant for SiO_2 (Fig. 6c) and TiO_2 (Fig. 6d) where a linear decrease in flotation rate constant is apparent with an increase in pH and NP dosage. This can be related to the reduction of selectivity with increasing NP dosage. A similar result for the influence of pH on flotation rate constant for γ-Al_2O_3 (Fig. 6a) and α-Fe_2O_3 (Fig. 6b) is observed, while by increasing the amount of NPs, the flotation rate constant increases for γ-Al_2O_3, α-Fe_2O_3 NPs as well. This increase can be attributed to high surface area and accessibility of attachment sites by increasing NPs amount. The reduction in flotation rate constant is linear in the Eqs. (4) and (13) and the same holds true in Fig. 6a and d.

3.5. Optimizing of RSM results

To study the flotation kinetic behaviour, the effects of different pHs and NP dosages, on the flotation rate constant were assessed, while Cu recovery (Y_1) and Cu grade (Y_2) remain most important objectives in optimization studies; therefore, only Y_1 and Y_2 are of concern. It should be noted that the optimized values of flotation rate constant for the NPs are approximately within the range of 0.82–1.05, such that the maximum value is obtained 1.05 for γ-Al_2O_3 NP. In our study, because the optimal value of the flotation rate constant is not the required response (the maximum recovery and grade values are the most important), and because with considering the optimal value, the desirability function value decreases; therefore, the effect of flotation rate constant was not considered.

The objective of RSM is to optimize the Y_1 and Y_2 values for both the independent parameters at different selected ranges in a simultaneous manner. Here, the pH and NP dosage values are maintained within the selected range of experimental condition. The optimal responses are obtained through the desirability function method, most widely applied in optimization of multiple response process in Design Expert software environment [42,43]. The optimum pHs and NP dosages in finding the maximum copper recovery and grade with the highest efficiency for these four NPs are tabulated in Table 12.

The confirmatory experiments are run through the recommended optimum conditions for all the NPs to check the model validity. The obtained results indicate that the copper recovery and grade are the highest for α-Fe_2O_3 and γ-Al_2O_3 NPs subject to optimum conditions pH = 12 and NP dosage = 6 kg/t, respectively. Because recovery is of high importance and also the grade is close to maximum value for α-Fe_2O_3 NP; therefore, this NP is recommended as having the best ability to improve column flotation performance.

Finally, it is important in this case to highlight that nanoparticles can greatly affect the froth phase. The experimental observations indicate that applying nanoparticles in the mineral flotation

lead to generation of many small bubbles in the froth phase and by preventing bubbles coalescence or burst, the froth is become more stable. It can be deduced that nanoparticles are highly contributive in having uniform bubble diameter and the recovery and flotation performance strongly depend on froth stability [27,28].

4. Conclusions

Here, the laboratory column flotation cell located at Sarcheshmeh Copper Complex is applied in assessing the effect of nanoparticles on the flotation performance through RSM technique. For this purpose, γ-Al_2O_3, α-Fe_2O_3, SiO_2 and TiO_2 nanoparticles due to their large possessing surface to volume ratio are selected as the froth stabilizers. The α-Fe_2O_3 NPs have the higher copper recovery, 71.30% at optimum experimental conditions, obtained through CCD method among its counterparts. The pH is a more effective parameter on all three responses, copper recovery, grade and flotation rate constant than NP dosage. For copper grade at optimum conditions, γ-Al_2O_3 NPs reveal optimal value of 29.81. However, α-Fe_2O_3 nanoparticle is recommended as having the best ability to improve column flotation performance. Assessing the flotation rate constant is run for evaluating the nanoparticle impact on flotation kinetic. The agreement between the actual and predicted values are acceptable, that is, their applicability in the mining industry. The results obtained here at optimum conditions indicate that these nanoparticles can be applied efficiently for mineral separation in industrial samples in general, but here, in specific, could increase copper recovery and grade.

Declaration of Competing Interest

The authors declare that they have no known competing financial interests or personal relationships that could have appeared to influence the work reported in this paper.

References

[1] Sarhan AR, Naser J, Brooks G. CFD model simulation of bubble surface area flux in flotation column reactor in presence of minerals. Int J Min Sci Technol 2018;28(6):999–1007.

[2] Azizi A, Ahmad H, Behnam F. Investigating the first-order flotation kinetics models for Sarcheshmeh copper sulfide ore. Int J Min Sci Technol 2015;25(5):849–54.

[3] Ahmadi R, Khodadadi DA, Abdollahy M, Fan M. Nano-microbubble flotation of fine and ultrafine chalcopyrite particles. Int J Min Sci Technol 2014;24(4):559–66.

[4] Shahbazi B, Rezai B, Chehreh Chelgani S, Koleini SMJ, Noaparast M. Estimation of diameter and surface area flux of bubbles based on operational gas dispersion parameters by using regression and ANFIS. Int J Min Sci Technol 2013;23(3):343–8.

[5] Ran J, Liu J, Zhang C, Wang D, Li X. Experimental investigation and modeling of flotation column for treatment of oily wastewater. Int J Min Sci Technol 2013;23(5):665–8.

[6] Wang J, Park H, Ng CY, Wang L. Use of oscillatory air supply for improving the throughput and carrying capacity of column flotation. Powder Technol 2019;353:41–7.

[7] Zanin M, Wightman E, Grano SR, Franzidis JP. Quantifying contributions to froth stability in porphyry copper plants. Int J Miner Process 2009;91(1–2):19–27.

[8] Farrokhpay S. The significance of froth stability in mineral flotation - A review. Adv Colloid Interface Sci 2011;166(1–2):1–7.

[9] Gupta AK, Banerjee PK, Mishra A, Satish P, Pradip. Effect of alcohol and polyglycol ether frothers on foam stability, bubble size and coal flotation. Int J Miner Process 2007;82(3):126–37.

Table 12
Most effective independent parameters applied in finding the optimum responses Y_1 and Y_2 for NPs.

Nanoparticle	X_1	X_2 (kg/t)	Y_1 (%)	Y_2 (%)	Desirability
γ-Al_2O_3	12.00	6	69.35	29.81	0.969
α-Fe_2O_3	12.00	6	71.30	27.06	0.963
SiO_2	11.96	6	65.80	26.00	0.964
TiO_2	11.33	6	65.06	25.49	0.785
Without NPs	N/A	N/A	62.00	24.78	N/A

[10] Nakhaei F, Mosavi MR, Sam A. Recovery and grade prediction of pilot plant flotation column concentrate by a hybrid neural genetic algorithm. Int J Min Sci Technol 2013;23(1):69–77.

[11] Nguyen AV, Schulze HJ. Colloidal science of flotation. New York: Marcel Dekker; 2004. p. 840.

[12] Pugh RJ. Experimental techniques for studying the structure of foams and froths. Adv Colloid Interface Sci 2005;114–115:239–51.

[13] Grau RA, Laskowski JS, Heiskanen K. Effect of frothers on bubble size. Int J Miner Process 2005;76(4):225–33.

[14] Schwarz S, Grano S. Effect of particle hydrophobicity on particle and water transport across a flotation froth. Colloids Surf, A 2005;256(2–3):157–64.

[15] Nguyen AV, Phan CM, Evans GM. Effect of the bubble size on the dynamic adsorption of frothers and collectors in flotation. Int J Miner Process 2006;79(1):18–26.

[16] Binks BP. Particles as surfactants - Similarities and differences. Curr Opin Colloid Interface Sci 2002;7(1–2):21–41.

[17] Horozov TS. Foams and foam films stabilised by solid particles. Curr Opin Colloid Interface Sci 2008;13(3):134–40.

[18] Cheng G, He M, Peng H, Hu B. Dithizone modified magnetic nanoparticles for fast and selective solid phase extraction of trace elements in environmental and biological samples prior to their determination by ICP-OES. Talanta 2012;88:507–15.

[19] Jiang HM, Yan ZP, Zhao Y, Hu X, Lian HZ. Zincon-immobilized silica-coated magnetic Fe$_3$O$_4$ nanoparticles for solid-phase extraction and determination of trace lead in natural and drinking waters by graphite furnace atomic absorption spectrometry. Talanta 2012;94:251–6.

[20] Sirota V, Selemenev V, Kovaleva M, Pavlenko I, Mamunin K, Dokalov V, et al. Preparation of crystalline Mg (OH)$_2$ nanopowder from serpentinite mineral. Int J Min Sci Technol 2018;28(3):499–503.

[21] Khaleghi A, Ghader S, Afzali D. Ag recovery from copper anode slime by acid leaching at atmospheric pressure to synthesize silver nanoparticles. Int J Min Sci Technol 2014;24(2):251–7.

[22] Hajati A, Shafaei SZ, Noaparast M, Farrokhpay S, Aslani S. Novel application of talc nanoparticles as collector in flotation. RSC Adv 2016;6(100):98096–103.

[23] Panneerselvam P, Morad N, Tan KA. Magnetic nanoparticle (Fe$_3$O$_4$) impregnated onto tea waste for the removal of nickel (II) from aqueous solution. J Hazard Mater 2011;186(1):160–8.

[24] Du Z, Bilbao-Montoya MP, Binks BP, Dickinson E, Ettelaie R, Murray BS. Outstanding stability of particle-stabilized bubbles. Langmuir 2003;19(8):3106–8.

[25] Dickinson E, Ettelaie R, Kostakis T, Murray BS. Factors controlling the formation and stability of air bubbles stabilized by partially hydrophobic silica nanoparticles. Langmuir 2004;20(20):8517–25.

[26] Liu Q, Zhang SY, Sun DJ, Xu J. Foams stabilized by Laponite nanoparticles and alkylammonium bromides with different alkyl chain lengths. Colloids Surf, A 2010;355(1–3):151–7.

[27] Cilek EC, Uysal K. Froth stabilisation using nanoparticles in mineral flotation. Physicochem Probl Mineral Process 2018;54(3):878–89.

[28] Cilek EC, Karaca S. Effect of nanoparticles on froth stability and bubble size distribution in flotation. Int J Miner Process 2015;138:6–14.

[29] Sakkas VA, Islam MA, Stalikas C, Albanis TA. Photocatalytic degradation using design of experiments: a review and example of the Congo red degradation. J Hazard Mater 2010;175(1–3):33–44.

[30] Ahmadi M, Vahabzadeh F, Bonakdarpour B, Mofarrah E, Mehranian M. Application of the central composite design and response surface methodology to the advanced treatment of olive oil processing wastewater using Fenton's peroxidation. J Hazard Mater 2005;123(1–3):187–95.

[31] Behera SK, Meena H, Chakraborty S, Meikap BC. Application of response surface methodology (RSM) for optimization of leaching parameters for ash reduction from low-grade coal. Int J Min Sci Technol 2018;28(4):621–9.

[32] Kumar S, Venugopal R. Performance analysis of jig for coal cleaning using 3D response surface methodology. Int J Min Sci Technol 2017;27(2):333–7.

[33] Wang JP, Chen YZ, Ge XW, Yu HQ. Optimization of coagulation-flocculation process for a paper-recycling wastewater treatment using response surface methodology. Colloids Surf, A 2007;302(1–3):204–10.

[34] Khataee AR, Kasiri MB, Alidokht L. Application of response surface methodology in the optimization of photocatalytic removal of environmental pollutants using nanocatalysts. Environ Technol 2011;32(15):1669–84.

[35] Ebrahimi B, Shojaosadati SA, Ranaie SO, Mousavi SM. Optimization and evaluation of acetylcholine esterase immobilization on ceramic packing using response surface methodology. Process Biochem 2010;45(1):81–7.

[36] Bezerra MA, Santelli RE, Oliveira EP, Villar LS, Escaleira LA. Response surface methodology (RSM) as a tool for optimization in analytical chemistry. Talanta 2008;76(5):965–77.

[37] Li Y, Cui F, Liu Z, Xu Y, Zhao H. Improvement of xylanase production by Penicillium oxalicum ZH-30 using response surface methodology. Enzyme Microb Technol 2007;40(5):1381–8.

[38] Ahmadi S, Manteghian M, Kazemian H, Rohani S, Towfighi Darian J. Synthesis of silver nano catalyst by gel-casting using response surface methodology. Powder Technol 2012;228:163–70.

[39] Uçurum M. Influences of Jameson flotation operation variables on the kinetics and recovery of unburned carbon. Powder Technol 2009;191(3):240–6.

[40] Savassi ON, Alexander DJ, Franzidis JP, Manlapig EV. An empirical model for entrainment in industrial flotation plants. Miner Eng 1998;11(3):243–56.

[41] Mason RL, Gunst RF, Hess JL. Statistical design and analysis of experiments: with applications to engineering and science. New York: John Wiley & Sons; 2003.

[42] Mahjub R, Dorkoosh FA, Amini M, Khoshayand MR, Rafiee-Tehrani M. Preparation, statistical optimization, and in vitro characterization of insulin nanoparticles composed of quaternized aromatic derivatives of chitosan. AAPS PharmSciTech 2011;12(4):1407–19.

[43] Chu T, Zhang Q, Li H, Ma WC, Zhang N, Jin H, et al. Development of intravenous lipid emulsion of tanshinone IIA and evaluation of its anti-hepatoma activity in vitro. Int J Pharm 2012;424(1–2):76–88.